Analytica Chimica Acta 686 (2011) 40–49

Contents lists available at ScienceDirect

Analytica Chimica Acta

journal homepage: www.elsevier.com/locate/aca

Trace elemental analysis of airborne particulate matter using dynamic reaction cell inductively coupled plasma – mass spectrometry: Application to monitoring episodic industrial emission events

K. Suresh Kumar Danadurai[a], Shankararaman Chellam[a,b,*], Cin-Ty Lee[c], Matthew P. Fraser[d]

[a] Department of Civil and Environmental Engineering, University of Houston, Houston, TX 77204-4003, United States
[b] Department of Chemical and Biomolecular Engineering, University of Houston, Houston, TX 77204-4004, United States
[c] Department of Earth Science, Rice University, Houston, TX 77005, United States
[d] School of Sustainability, Arizona State University, Tempe, AZ 85287, United States

ARTICLE INFO

Article history:
Received 25 August 2010
Received in revised form
13 November 2010
Accepted 18 November 2010
Available online 26 November 2010

Keywords:
Atmospheric particulate matter
Dynamic reaction cell
ICP-MS
Rare earth elements
Industrial air pollution
Trace elements

ABSTRACT

The elemental composition of airborne particles is being increasingly monitored since several metals have been implicated in adverse human health outcomes and environmental deterioration while simultaneously providing clues to the identity and strength of their emission sources. However, quantification of several elements and transition metals in ambient aerosols, which are typically present only at trace levels, is fraught with interferences using quadrupole inductively coupled plasma – mass spectrometry (q-ICP-MS). We report improved measurements of key aerosol elements including Al, V, Cr, Fe, Ni, Cu, and Zn in airborne coarse particulate matter (PM_{10}) by exploiting ion-molecule reactions in a dynamic reaction cell (DRC) with NH_3 as the cell gas. Numerous other elements (Na, Mg, Si, K, Ca, Sc, Ti, Mn, Co, Ga, As, Se, Rb, Sr, Zr, Mo, Cd, Sn, Sb, Cs, Ba, Pb, Th, and U) and lanthanoids (Y, La, Ce, Pr, Nd, Sm, Eu, Gd, Tb, Dy, Ho, Er, Tm, Yb, and Lu), which are important trace components used for source apportionment studies, were also measured. Inter-laboratory comparison using sector field ICP-MS demonstrated the accuracy and precision of DRC-q-ICP-MS. This technique was used to determine the elemental composition of over 150 PM_{10} samples collected from an industrialized region in Houston, TX. Samples were first digested using a combination of HF, HNO_3, and H_3BO_3 in two stages in a microwave oven each with set points of 200 °C, 1.55 MPa (225 psig), and 20 min dwell time. Trace metals were used to identify an episodic release of particles from a local source and subsequently track the atmospheric transport of the released particles. This establishes the inherent value of such measurements to developing air quality management strategies since emission events can significantly worsen air quality over a large area. Based on our findings, we recommend continuous independent monitoring of emissions to augment existing industry self-reporting regulatory requirements. Such environmental measurements will assist in establishing industrial regulatory compliance while simultaneously providing data necessary to develop scientifically defensible air quality management strategies.

1. Introduction

Atmospheric particulate matter contributes to visibility reduction, climate change, cardiopulmonary and respiratory disease, and decreased life expectancy [1,2]. A portion of the toxicological or epidemiological response is thought to arise from the metals contained in the particles, which has been termed as the "metals hypothesis". For example, fine particulate Zn has been correlated with emergency department visits in Spokane, WA [3]. Particulate transition metals have also been correlated with increasing toxicity biomarkers and shown to stimulate production of reactive oxygen species [4]. Additionally, particulate metals can be used to identify sources and develop control strategies. Hence, establishing the elemental composition of atmospheric particles is essential to quantify the sources and health impacts of particulate air pollution. However, the inherent variability and heterogeneity of airborne particulate matter coupled to the very low sampled mass of metals complicate their reliable measurement.

* Corresponding author at: Department of Civil and Environmental Engineering, University of Houston, Houston, TX 77204-4003, United States.
Tel.: +1 713 743 4265; fax: +1 713 743 4260.
E-mail address: chellam@uh.edu (S. Chellam).

0003-2670/$ – see front matter © 2010 Elsevier B.V. All rights reserved.
doi:10.1016/j.aca.2010.11.037

Energy dispersive X-ray fluorescence (ED-XRF) has been traditionally employed for elemental analysis of aerosols collected on filters [5]. ED-XRF is well suited for routine measurements (e.g. for regulatory compliance) since it can provide multi-element data at very high throughput, with minimal labor, and without destroying the sample. Recently, elemental concentrations in ambient aerosols are being preferentially measured using inductively coupled plasma – quadrupole mass spectrometry (q-ICP-MS) since it (i) provides lower detection limits, (ii) is sensitive to a wider range of elements, (iii) is capable of high throughput, and (iv) has a linear dynamic range spanning several orders of magnitude [6–9]. However, trace level measurements of certain elements using this technique can be challenging due to mass spectral overlaps. But, plasma-based isobaric interferences and spectral overlaps from polyatomic species can be significantly suppressed by promoting ion-molecule reactions in a dynamic reaction cell (DRC) pressurized with a reactive gas. Technological improvements have allowed the incorporation of DRCs in commercially available ICP-MS instruments [10] facilitating trace level elemental measurements in a variety of sample matrices.

Enhanced measurements of several metals (Al, Co, Cr, Cu, Fe, Mn, Ni, Se, V, and Zn) have been reported in biological, environmental, and geological matrices using NH_3, H_2, CH_4, and O_2 as reaction cell gases [11–15]. The reaction cell approach has also been used for studying single elements in aerosols; for example, Cr [16] and Pt [17] and multiple elements [18,19] without providing details of the optimization of instrumental procedures and settings. To our knowledge, only one study has reported DRC optimization procedures in detail (including cell gas flow rate and bandpass parameter) for multi-elemental analysis in airborne particulate matter [20]. Lamaison et al. [20] collected aerosol samples from an industrialized region on the northern coast of France over 15-day periods. However, greater time resolution ($\leq$1 day) is typically necessary for source apportionment in urban locations where transient emissions and meteorological mixing are important (as will be discussed later in this paper). Also, extractions were performed with a HCl–HNO_3–HF mixture, even though HCl is typically not employed for atmospheric particles unless platinum group elements are targeted, e.g. [7–9,21]. Further, not using H_3BO_3 may have reduced certain elemental recoveries due to loss as fluoride precipitates [8,21]. Hence, additional research is necessary to evaluate the applicability of DRC to measure particulate metals under conditions more closely applicable to low mass/high time resolution sampling where only approximately 200 μg of tropospheric aerosol samples is typically collected and extracted in the absence of HCl (using HNO_3–HF–H_3BO_3).

The principal objective of this research is to develop a DRC-q-ICP-MS technique for the multi-elemental analysis of ambient atmospheric particulate matter, which is necessary for source separation when a variety of emission sources exist. NH_3 was selected as the reaction gas since it is widely used for suppressing interferences for a number of elements [22]. A total of 154 aerosol samples were first digested in a microwave oven with HNO_3, HF, and H_3BO_3. A total of 31 main group and transition metals (Na, Mg, Al, Si, K, Ca, Sc, Ti, V, Cr, Mn, Fe, Co, Ni, Cu, Zn, Ga, As, Se, Rb, Sr, Zr, Mo, Cd, Sn, Sb, Cs, Ba, Pb, Th, and U) as well as 15 lanthanoids (Y, La, Ce, Pr, Nd, Sm, Eu, Gd, Tb, Dy, Ho, Er, Tm, Yb, and Lu) were quantified. Concentrations of several elements including those that were more accurately measured with the DRC technique (Al, V, Cr, Fe, Ni, Cu, and Zn) were independently validated using sector field ICP-MS in a different laboratory. Results reported herein are part of our larger effort aimed at studying air quality in Southeast Texas including the Houston–Galveston metropolitan area. We are particularly interested in identifying the chemical composition of primary emissions of particles, mechanisms of secondary particle formation including metal-catalyzed heterogeneous reactions leading to sulfate aerosols, and whether industry-self reporting of episodic emissions from transient operation in the region's refineries and petrochemical plants accurately describes their local environmental impact.

2. Experimental

2.1. Ambient aerosols

Particles with aerodynamic diameter <10 μm (PM_{10}) were collected on 47-mm diameter Teflon membrane filters at a flow rate of 1 $m^3\ h^{-1}$ over 3- or 6-h intervals between April 30, 2009 and May 27, 2009. This campaign was coordinated with the Study of Houston Atmospheric Radical Precursors (SHARP) fieldwork to provide data regarding potential heterogeneous reactions which play an important role in radical formation (especially HONO, HCHO, and $ClNO_2$). Two Rupprecht & Patachnick (R&P) 2025 samplers (Thermo Scientific Corporation) were deployed at Clinton Drive, Houston, TX (latitude +29.733611 and longitude −95.257500). This continuous ambient monitoring (CAM) site is operated by the Texas Commission on Environmental Quality (TCEQ) and is located near the heavily industrialized Houston Ship Channel. Of significant concern to the State of Texas is that fine and coarse PM concentrations are close to regulatory limits, thereby focusing attention on local and regional particle sources to determine the most effective means to reduce local aerosol concentrations. After sample collection, filters were sealed inside Petri dishes and frozen until further analysis.

2.2. Instrumentation

2.2.1. Closed vessel microwave-assisted acid digestion

Our previously developed two-stage microwave digestion (MARS 5, CEM Corp., Matthews, NC) procedure was employed for all samples [21,23]. In the first stage, the PM_{10} sample along with 3 mL HNO_3 (14.3 M) and 10 μL HF (48%) was heated to 200 °C at a pressure set point of 1.55 MPa (225 psig) for a dwell time of 20 min. In the second stage, 80 μL of 5% (*m*/*v*) H_3BO_3 was added before reheating at the same microwave settings to mask any remaining HF and redissolve fluoride precipitates. After cooling, the resulting digestate was diluted with ultrapure water to a final 1 M concentration of HNO_3 prior to ICP-MS. Acid volumes were proportionately increased (0.3 mL HF, 3 mL HNO_3, and 2.4 mL H_3BO_3) for analysis of the higher masses used in SRM analysis (10 mg). The instrument was programmed in the "standard control" mode and pressure and temperature profiles in the master vessel were always monitored separately on a personal computer. In all cases, the 200 °C set-point was reached first and temperature remained the primary controlling parameter throughout the programmed dwell time of 20 min in both stages.

2.2.2. DRC-q-ICP-MS

A quadrupole ICP-MS system fitted with a dynamic reaction cell (Elan DRC II, PerkinElmer SCIEX) was employed for elemental analyses. Instrumental characteristics and operating parameters are summarized in Table 1. Daily optimization was performed using a Smart Tune solution (PerkinElmer) consisting of 10 μg L^{-1} Ba, and 1 μg L^{-1} Be, Mg, Fe, Co, In, Ce, Pb, Th, and U. Formation of oxides ($^{156}CeO^+/^{140}Ce^+ < 2\%$) and doubly charged ions ($^{138}Ba^{2+}/^{138}Ba^+ < 2.4\%$) was minimized by adjusting nebulizer gas flow. Auto lens voltage was adjusted to maximize ion transmission based on ^{9}Be, ^{59}Co, and ^{115}In. Under typical operating conditions, sensitivities for ^{24}Mg, ^{115}In, and ^{238}U were $\sim 10^4$, $\sim 4 \times 10^4$, and 3×10^4 cps ppb^{-1}, respectively. Calibration was performed with two multi-element standards; the first one contained Na, Mg, Al, K, Ca, Sc, Ti, V, Cr, Mn, Fe, Co, Ni, Cu, Zn, Ga, As, Se, Rb, Sr, Zr, Mo, Cd,

Table 1
Instrument settings for dynamic reaction cell q-ICP-MS.

Instrument	Elan DRC II (PerkinElmer SCIEX)
Nebulizer	Concentric (Meinhard)
Spray chamber	Baffled quartz cyclonic
Torch injector	Quartz
Auto lens	On
RF power	1300 W
Gas flow rates	
Plasma	16 L min^{-1}
Nebulizer	1.0–1.04 L min^{-1}
Auxiliary	1 L min^{-1}
Interface	Platinum cones
Sampler	1.1 mm diameter
Skimmer	0.9 mm diameter
Measurement parameters	
Scanning mode	Peak hopping
Sweeps/reading	20
Readings/replicate	1
Replicates	3
Dwell time	50 ms (standard mode); 100 ms (DRC mode)
Sampling parameters	AS-93plus autosampler
Sample flush time	35 s
Sample flush pump speed	24 rpm
Read delay	65 s
Read delay pump speed	20 rpm
Wash time	60 s
Wash pump speed	24 rpm
DRC parameters	
Cell gas	NH_3 (0.35–0.75 mL min^{-1})
RPq	0.3–0.65
RPa	0

Sn, Sb, Cs, Ba, Pb, Th, and U and the second one contained the lanthanoids (Y, La, Ce, Pr, Nd, Sm, Eu, Gd, Tb, Dy, Ho, Er, Tm, Yb, and Lu). Silicon was measured separately since it was present in very high concentrations. Platinum cones were cleaned using a detergent and 2% HNO_3 by ultrasonication for 5 min approximately once every 30 filter samples or when ^{115}In sensitivity was decreased by ~25%.

To evaluate the DRC performance, differences in signal intensities between a matrix matched blank solution (3 mL of 65% HNO_3, 10 μL of 48% HF and 80 μL of 5% H_3BO_3) with and without a 1 μg L^{-1} spike of the analyte of interest were compared. Comparisons were also made with the blank and a 15× diluted digestate of a particulate matter filter sample. Ion intensities were measured by varying the NH_3 flow rate between 0.1 and 1 mL min^{-1} at a fixed mid-range RPq setting of 0.45. NH_3 was the only cell gas evaluated in this research given its high reactivity (since its ionization energy is high (10.2 eV) but lower than that of argon (15.8 eV)), and widespread use [22]. The optimal cell gas flow was chosen corresponding to the minimum background equivalent concentrations obtained during these measurements. The RPq value was optimized next in a similar manner by holding the NH_3 gas flow rate at the optimal value determined earlier but varying the RPq in the range 0.1–0.85. The RPa was held constant at 0.

^{7}Li, ^{74}Ge, ^{103}Rh, ^{115}In and ^{209}Bi (1 μg L^{-1}, High Purity Standards, Charleston, SC) spiked in all calibration standards and samples were initially evaluated as potential internal standards to correct non-spectral interferences. Accurate and precise measurements of all certified and uncertified elements from NIST Standard Reference Materials (SRM 1648 and SRM 1648a) were possible using ^{115}In for lanthanoids and metals measured using the reaction cell (see Section 3.1). Other elements were corrected using ^{74}Ge (Na, Mg, K, Mn, and Co) and ^{103}Rh (Sr, Zr, and Mo) and ^{115}In (As, Ga, Rb, Sb, Pb, Th, and U).

2.2.3. Sector field ICP-MS

Measurements in the Department of Earth Sciences at Rice University were done on a ThermoFinnigan Element 2 magnetic sector, single-collector ICP-MS with reverse magnetic and electrostatic geometry. Samples were introduced into a small-volume cyclonic spray chamber with an Elemental Scientific Teflon nebulizer using free aspiration with an uptake rate of ~100 μL min^{-1}. A Pt guard electrode and a high sensitivity Ni skimmer cone were used. Relevant parameters were 13.4 L min^{-1} of Ar cool gas, 0.94 L min^{-1} of Ar sample gas, and 0.97 L min^{-1} of Ar carrier ("auxillary") gas. Forward power was 1370 W and reflected power was 2 W. All analyses were run in medium mass resolution mode, $m/\Delta m = 4000$ (as defined by the width of the peak between 10% shoulder heights), which was sufficient to resolve all isobaric interferences (argides, oxides, and double-charged ions) relevant to the elements of interest. The sensitivity of the instrument in medium mass resolution mode for 1 μg L^{-1} of ^{115}In was 150,000 cps. Long-term drift of the magnet was corrected for by centering on the $^{40}Ar^{40}Ar^{+}$ during each run. Small peak offsets associated with differences in magnet hysteresis between the mass calibration and actual measurements were empirically corrected for using instrument software. All masses were thus fully centered during analyses. The following masses were measured: ^{23}Na, ^{24}Mg, ^{27}Al, ^{44}Ca, ^{49}Ti, ^{51}V, ^{52}Cr, ^{53}Cr, ^{55}Mn, ^{56}Fe, ^{57}Fe, ^{59}Co, ^{60}Ni, ^{65}Cu, ^{66}Zn, ^{68}Zn, and ^{115}In. Two isotopes for Cr, Fe and Zn were measured to double-check against polyatomic interferences: in all cases, mass ratios 52/53, 56/57, and 66/68, matched the accepted isotopic compositions of Cr, Fe and Zn, respectively, to within 5%. For each peak, we scanned a 150% mass window (defined as $\Delta m/m \times 100$), which insured that the entire peak was captured. The peak was then centered again using automated instrument software and then the signal within an 80% mass window centered on the peak was integrated. Each peak involved 15 measurement slices, each with a dwell time of 0.01 s for a total peak dwell time of 0.15 s. Mass scans from mass 23 to 115 required changing the magnet current 7 times (with a magnetic delay time of 0.034 s) in between which mass scans were done by changing the electrostatic field at constant magnetic current. A total of 30 runs across the entire mass range were measured.

2.3. Reagents and reference materials

65% HNO_3 and 99.999% H_3BO_3 (EM Science, Gibbstown, NJ) and 48% HF (Fluka, Milwaukee, WI) were employed for digestions. High purity water with 18.2 MΩ cm resistivity and dissolved organic carbon concentration <3 μg L^{-1} (Max159 Modulab, U.S. Filter Corporation, Lowell, MA) was used for all cleanings, dilutions, and solution preparations. Identical concentrations were maintained in the background matrix (HNO_3–HF–H_3BO_3) of reagent blank solutions, calibrations standards, and sample digestates to minimize errors related to matrix inconsistencies. Instrumental drift and plasma fluctuations were corrected using internal standards (1 μg L^{-1} ^{74}Ge and ^{115}In). SRM 1648 and SRM 1648a (urban particulate matter) reference materials were used for initial experiments to determine the accuracy and precision of our procedures. The cell gas (99.999% NH_3) was purchased from Matheson Trigas.

2.4. Isotope selection

^{23}Na, ^{27}Al, ^{55}Mn, ^{59}Co, ^{75}As, ^{89}Y, ^{141}Pr, ^{159}Tb, ^{165}Ho, ^{169}Tm, and ^{232}Th were monitored since they are monoisotopic. For all other elements, at least two isotopes were initially monitored in reference materials and quality control standards. Appropriate isotopes were selected based on the accuracy of agreement between measured elemental concentrations with those reported in SRMs and the spiked value in the quality control sample. Wherever possible, the most abundant isotope was selected (^{24}Mg, ^{39}K, ^{51}V, ^{52}Cr, ^{63}Cu, ^{69}Ga, ^{85}Rb, ^{88}Sr, ^{90}Zr, ^{98}Mo, ^{121}Sb, ^{139}La, ^{140}Ce, ^{153}Eu, ^{166}Er, ^{175}Lu, ^{208}Pb, and ^{238}U). Less abundant isotopes were chosen for the remaining elements measured to reduce isobaric and polyatomic mass spectral interferences (^{44}Ca, ^{47}Ti, ^{57}Fe, ^{60}Ni, ^{66}Zn, ^{82}Se,

^{111}Cd, ^{137}Ba, ^{146}Nd, ^{147}Sm, ^{157}Gd, ^{163}Dy, and ^{172}Yb). ^{57}Fe also provided improved detection limits and accurate measurements were possible using this least abundant isotope as Fe concentrations were sufficiently high in the aerosol samples. Similar to earlier observations [24], anomalously high background (approximately 100,000 cps) at m/z of 68 were obtained when NH_3 was introduced in the reaction cell disallowing monitoring of ^{68}Zn in the DRC mode.

3. Results and discussion

3.1. Identification of elements to be measured using the reaction cell

Quantitative recoveries for all certified and non-certified elements were obtained for both SRM 1648 (91–110%) and SRM 1648a (90–104%) even in the "standard" mode of operation, i.e. absence of NH_3 (see Supplemental Data). It should be noted that these experiments were performed using 10 mg of SRM (to avoid heterogeneity problems), which is approximately 50 times the mass of aerosols in the actual PM_{10} samples. Hence, these results demonstrate the validity of our microwave extraction procedure and ICP-MS protocols only for relatively high analyte concentrations. Additionally, even though these SRMs are valuable tools for method development targeted towards atmospheric particles, their elemental composition does not always closely correspond to urban aerosols from different locations. Further, the 90th percentile size of SRM 1648a is 30.1 μm, which is 3 times larger than the maximum size of sampled aerosols (10 μm). Therefore, to develop and evaluate ICP-MS protocols more closely applicable to PM_{10}, three separate measurements were considered. First, SRM 1648 and SRM 1648a digestates were further diluted to bring elemental concentrations in the expected range for actual PM_{10} samples prior to ICP-MS measurements. For several elements, spike (1 μg L^{-1}) recoveries from 5 different PM_{10} samples and measurements of 12 separate standard solutions (1 μg L^{-1} and 5 μg L^{-1}) introduced after every 10 sample injections were also monitored.

A 900× dilution of SRM1648a digestate was made to bring V and Cr concentrations (0.247 and 0.781 μg L^{-1}, respectively) in the same range (0.035–4.56 for Cr and 0.029–3.63 μg L^{-1} for V) as PM_{10} samples diluted to 1 M HNO_3 as needed for ICP-MS analysis. Under these conditions, V and Cr recoveries were unacceptably low (only 65% and 70%, respectively) in the standard mode whereas utilizing NH_3 improved recoveries to 96.5% and 102.6%, respectively, in the DRC mode. Additionally, recoveries of spikes and standards were nearly quantitative and varied in a narrower range around 100% in the DRC mode compared with the standard mode for Al, V, Cr, Fe, Ni, Cu, and Zn. For example, spike recoveries in the DRC mode for Al and Fe were 99.0 ± 7.81% and 110 ± 9.93%, respectively, whereas it was 116 ± 6.25% and 126 ± 18.9%, respectively, in the standard mode. Similarly, using the reaction cell, recoveries of Ni, Cu, and Zn standard solutions were 101 ± 4.49%, 98.3 ± 5.00%, and 100. ± 9.07%, respectively, whereas it was 93.5 ± 5.66%, 94.6 ± 5.88%, 98.4 ± 15.9%, respectively, in the standard mode. Hence, more accurate and precise measurements for seven metals (Al, V, Cr, Fe, Ni, Cu, and Zn) were made using the reaction cell.

3.2. Selection of DRC parameters

3.2.1. NH_3 flow rate optimization

Introducing NH_3 suppressed signal intensities in the blank solution by 1–2.5 orders of magnitude for the elements of interest (e.g. 5000 to ~50 cps for m/z 57 and 1000 to ~100 cps for m/z 66 and 60). Importantly, the background signals for m/z 51 and 52 were nearly eliminated by NH_3 (~5 and 100 cps, respectively) allowing ultra-trace determination of ^{51}V and ^{52}Cr in airborne particulate matter samples in the DRC mode.

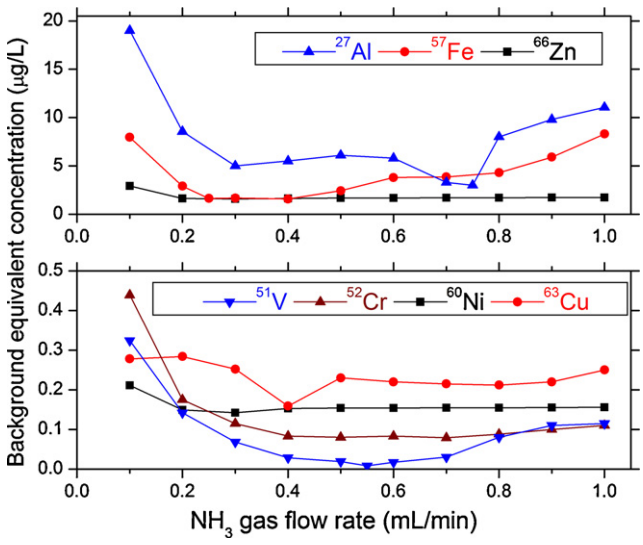

Fig. 1. NH_3 flow rate optimization for the dynamic reaction cell.

Fig. 1 shows changes in the background equivalent concentration (BEC) obtained by recording ion intensities (cps) for both background and spiked samples for Al, V, Cr, Fe, Ni, Cu and Zn by varying the NH_3 flow rate between 0.1 and 1 mL min^{-1} when RPq was set at 0.45. Decreasing BECs can be observed for different elements in the NH_3 flow rate range 0.30–0.75 mL min^{-1}, which can be attributed to removal of interferences through ion-molecule collisions before ions enter the mass analyzer. Fast electron transfer (or charge exchange) reactions between NH_3 and the polyatomic or isobaric interfering species in the reaction cell is the principal reason for improvements in detection [10,22]:

$$P^+ + NH_3 \rightarrow P + NH_3^+ \quad (\text{e.g. } P = {}^{40}Ar^{12}C \text{ for } {}^{52}Cr \text{ and } {}^{35}Cl^{16}O \text{ for } {}^{51}V)$$

Signal loss for the analyte through condensation and clustering reactions with NH_3 or due to scattering also occurs simultaneously, but at a lower kinetic rate thereby allowing measurement using the reaction cell:

$$M^+ + NH_3 \rightarrow MNH^+ + H_2 \quad (\text{e.g. } M = Cu, Zn, \text{ and } V)$$

As seen in Fig. 1, BECs decreased only slightly for Ni, Cu, and Zn indicating that their measurements could be made in a wide range of NH_3 flow rates. The lowest NH_3 flow rate corresponding to the minimum BEC for each of these elements was selected and is summarized in Table 2.

Background counts at m/z 27 were very similar for HNO_3 alone and the mixed acids HNO_3 + HF + H_3BO_3. NH_3 flow rate optimization was performed for both acid solutions (RPq = 0.45) but similar results were obtained in terms of background reduction in both cases. Similar behavior was observed even at a higher RPq setting of 0.65. Hence, ^{27}Al interferences appear to arise not only from boron (hydr)oxides but also from $^{12}C^{15}N$, $^{13}C^{14}N$, $^{12}C^{14}N^1H$, and $^{54}Fe^{2+}$.

3.2.2. RPq optimization

Even trace impurities in the cell gas can give rise to significant unintended interferences within the reaction cell. However, these polyatomic reaction products can be ejected before entering the mass analyzer by adjusting the bandpass of the reaction cell quadrupole. Fig. 2 shows the DRC optimization of the bandpass rejection parameter q (RPq) for V, Cr, Ni, and Cu. The RPq value was varied from 0.1 to 0.85 while maintaining the optimum NH_3

Table 2
Summary of dynamic reaction cell measurements.

Element	Major polyatomic interferences[a]	DRC parameters		Method detection limit ($\mu g L^{-1}$)		Accuracy with SRM1648 ($\mu g g^{-1}$)		Accuracy with SRM1648a ($\mu g g^{-1}$)	
		NH_3 flow rate ($mL min^{-1}$)	RPq value	Standard mode	DRC mode	Our study	Certified value	Our study	Certified value
^{27}Al	$^{11}B^{16}O$, $^{10}B^{16}O^{1}H$, ^{54}Fe, $^{12}C^{15}N$, $^{13}C^{14}N$, $^{12}C^{14}N^{1}H$	0.75	0.50	1.812	1.114	37,700 ± 4060	34,200 ± 1100	33,500 ± 534	34,300 ± 1300
^{51}V	$^{35}Cl^{16}O$, $^{36}Ar^{14}NH$, $^{36}Ar^{15}N$, $^{34}S^{16}O^{1}H$	0.55	0.50	0.083	0.014	130 ± 12	127 ± 7	125 ± 9	127 ± 11
^{52}Cr	$^{40}Ar^{12}C$, $^{36}Ar^{16}O$, $^{38}Ar^{14}N$, $^{35}Cl^{17}O$, $^{37}Cl^{15}N$, $^{35}Cl^{16}O^{1}H$	0.55	0.50	0.069	0.012	412 ± 1	403 ± 12	392 ± 3	402 ± 13
^{57}Fe	$^{40}Ar^{16}O^{1}H$, $^{40}Ca^{16}O^{1}H$	0.40	0.75	1.027	0.211	39,400 ± 3300	39,100 ± 1000	37,400 ± 2300	39,200 ± 2100
^{60}Ni	$^{44}Ca^{16}O$, $^{23}Na^{37}Cl$, $^{36}Ar^{24}Mg$	0.30	0.30	0.121	0.074	86 ± 2	82 ± 3	81 ± 2	81.1 ± 6.8
^{63}Cu	$^{40}Ar^{23}Na$, $^{35}Cl^{14}N_2$, $^{31}P^{16}O_2$	0.40	0.40	0.095	0.075	622 ± 20	609 ± 27	580 ± 25	610 ± 70
^{66}Zn	$^{50}Ti^{16}O$, $^{31}P^{17}O_2{}^{1}H$, $^{33}S_2$, $^{34}S^{16}O_2$, $^{40}Ca^{16}O$	0.35	0.30	0.143	0.122	4730 ± 202	4760 ± 140	4600 ± 234	4800 ± 270

Accuracy characterized by comparing certified concentrations provided by NIST and three separate measurements over the duration of this study.
[a] From Ref. [22] and references within.

gas flow for each element obtained in the previous section. The optimum RPq value corresponds to the maximum ratio of signal to background intensities for each element, which is also summarized in Table 2. The improvements observed in most cases (except for Ni) were caused by steep reductions in background counts which were low (<1000) to begin with even at RPq of 0.1. In contrast, while Ni background and signal intensities were comparable at low RPq, an increase in RPq from 0.1 to 0.3 caused the background to reduce by nearly 300-fold with only a corresponding 50-fold reduction in signal intensity. Hence, the RPq value is vital for effective measurement of Ni in airborne particles. Since the RPq did not significantly influence signal to background ratios for Al, Fe, and Zn they are not shown here.

The optimum NH_3 flow rate and RPq value for each element did not vary significantly over the course of this research and hence the values given in Table 2 were employed for all samples.

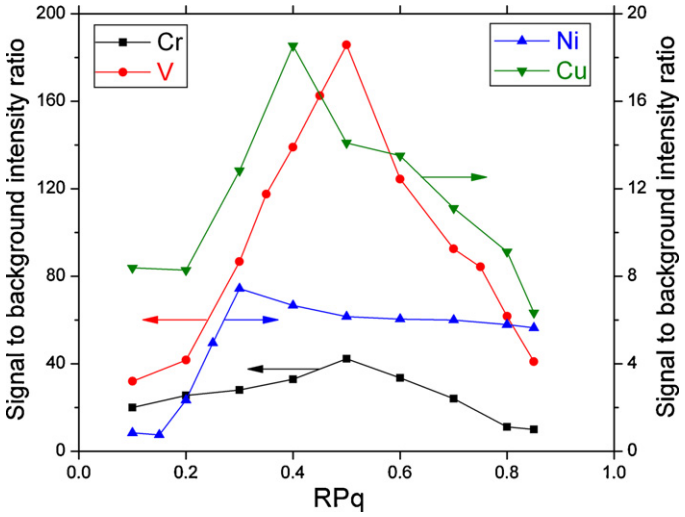

Fig. 2. RPq optimization for the dynamic reaction cell.

Table 3
Effect of NH_3 on signal to blank intensity ratios for the 5 $\mu g L^{-1}$ calibration standard.

	Al	V	Cr	Mn	Fe	Ni	Cu	Zn	As	Cd
DRC mode[a]	22	1598	83	70	35	32	48	20	656	949
Standard mode	12	61	8	123	6	20	33	9	766	3429

[a] NH_3 flow and RPq settings as in Table 2.

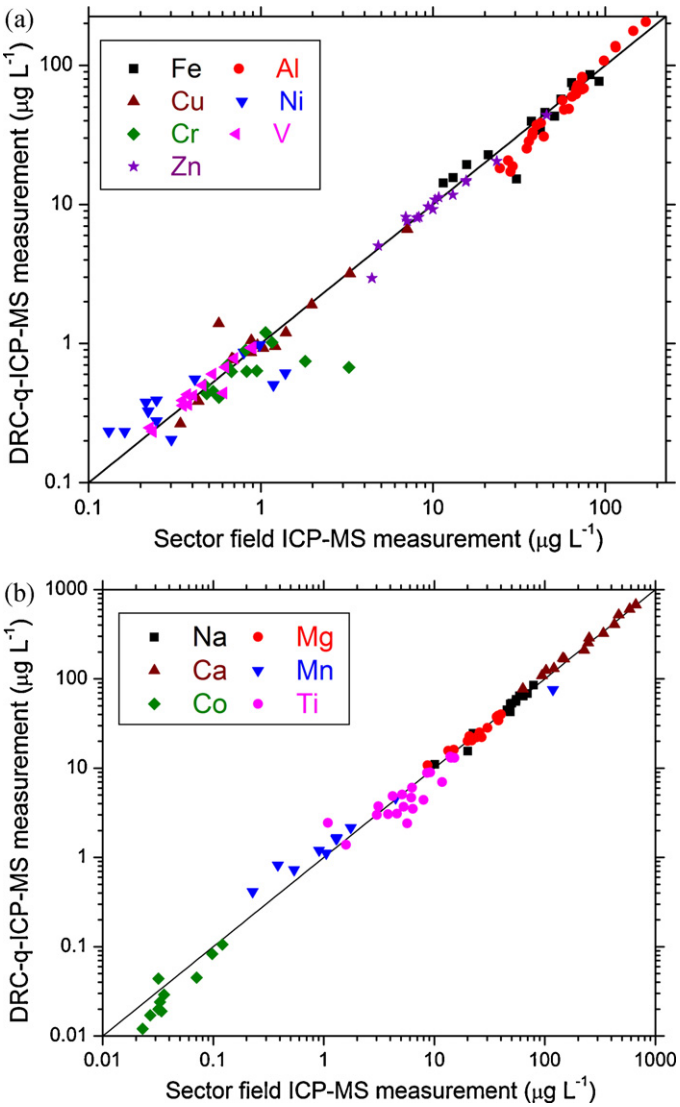

Fig. 3. Scatter plots of elemental concentrations measured using q-ICP-MS and sector field ICP-MS. The solid line denotes perfect equality between the two measurement techniques.

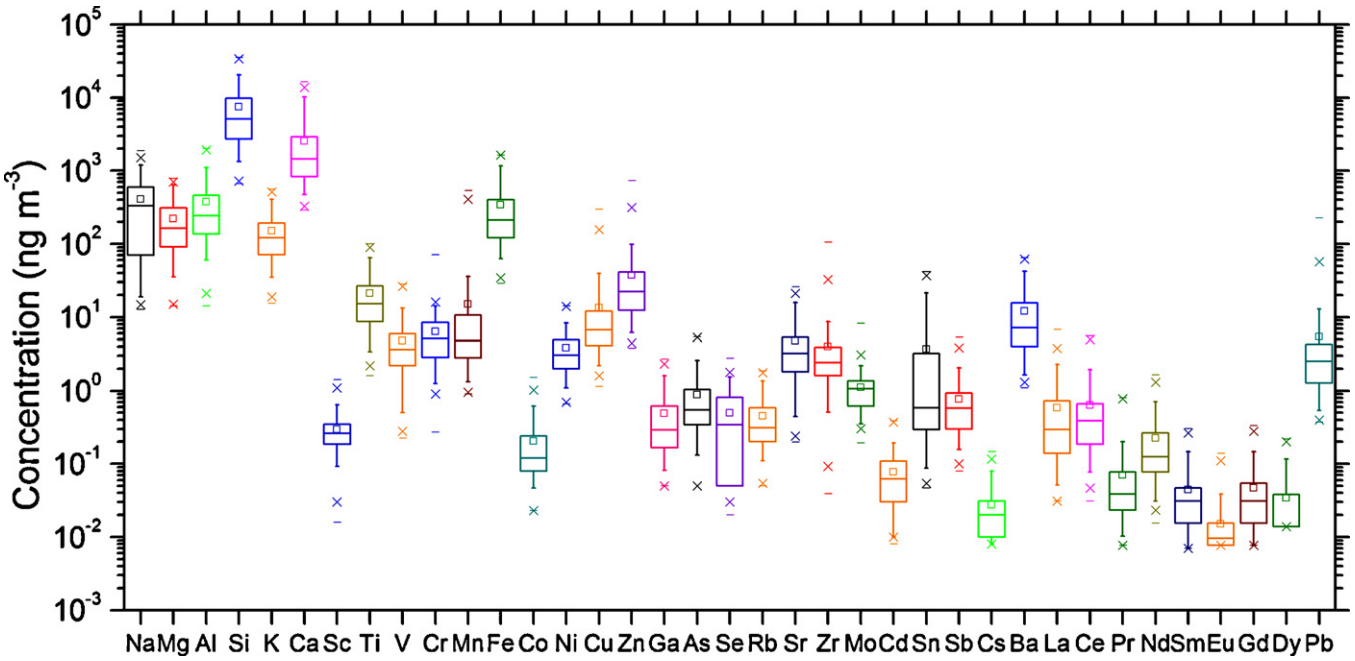

Fig. 4. Elemental composition of 154 samples of ambient airborne PM_{10} particles collected in an industrialized area in Houston, TX. The box encompasses the 25th and 75th percentiles and the whiskers are determined by the 5th and 95th percentiles. The horizontal line inside the box is the median and the open square is the average. Crosses (×) denote 1st and 99th percentiles and the maximum and minimum values are represented by dashes (–).

3.2.3. Detection limits

Method detection limits (MDLs) were determined following consecutive analysis of 10 replicates of spiked (10 ng L^{-1} to 1 μg L^{-1}) standards in the matrix matched blank solution (Table 2). Using the reaction cell decreased MDLs for the corresponding elements since introducing NH_3 reduced the background signal substantially (especially for V and Cr where the background signal was only ~5 cps). Poor MDLs for Al is attributed to high blank intensities obtained at m/z 27 (see Section 3.2.1).

3.2.4. Quality assurance

No statistically significant differences ($p = 0.05$) in SRM elemental concentrations were observed when digestions and DRC-q-ICP-MS measurements were repeated on three different dates during the course of this research. Recoveries of the elements measured in the DRC mode were 95–110% confirming accurate digestions and ICP-MS measurements (see Table 2). Post-digestion spike recoveries for all these elements from SRMs, filters, and standards were also satisfactory (83–110%) further confirming accurate elemental measurements

As shown in Table 3, signal to blank ratios for ^{51}V and ^{52}Cr increased favorably (by a factor of 26 and 10, respectively) under optimized DRC parameters. A lower magnitude of increase (1.6–5.8-fold) was observed for ^{27}Al, ^{57}Fe, ^{60}Ni, ^{63}Cu, and ^{66}Zn. Hence, it is emphasized that NH_3 was employed for PM_{10} samples fully expecting modest improvements for Al, Fe, Ni, Cu, and Zn, whereas substantially better measurements were achieved for V and Cr. In contrast, corresponding ratios for Mn, As, and Cd were <1 making the measurement of these elements by the standard method preferable.

3.3. Method validation by comparison of q-ICP-MS with sector field ICP-MS

Comparisons of elemental concentrations in selected PM_{10} samples obtained by q-ICP-MS at the University of Houston and by sector field ICP-MS at Rice University are presented in Fig. 3 in the form of bivariate scatter plots. Fig. 3a depicts elements measured in the DRC mode whereas Fig. 3b summarizes results for elements for which NH_3 was not necessary (standard mode). Paired t-tests, regression analysis, and non-parametric Wilcoxon signed-rank tests revealed no statistical differences between the two methods at 95% confidence for all these elements with the exception of Co. As observed in Fig. 3b, Co was present in very low concentrations (2–100 ng L^{-1}) compared with all other elements. Both instruments accurately measured Co in SRM 1648a at a higher concentration ~150 ng L^{-1}. Hence, elemental concentrations in aerosol samples measured by q-ICP-MS were accurate and precise and can be used as the scientific basis for environmental policy decisions.

3.4. Elemental composition of ambient PM_{10} samples

Fig. 4 summarizes concentrations of 37 elements which were consistently detected above their respective detection limits in PM_{10}. Heavy REEs (Tb, Ho, Er, Tm, Yb, and Lu), Th, and U are not depicted since these elements were measured above their detection limits in only 3–25% of the samples. Elemental concentrations varied by 1–2 orders of magnitude in the atmosphere reflecting the inherent variability in particulate emissions of contributing sources and meteorology. As may be expected, crustal elements, viz. Na, Mg, Al, K, Ca, Ti, Si, and Fe were dominant. A few main group and transition metals (Co, Ga, Se, Rb, Cd, Sn, Sb, and Cs) and lanthanoids (Pr, Nd, Sm, Eu, Gd, and Dy) were detected at ultra-trace (pg m^{-3}) levels in several samples.

Enrichment factors of individual elements (X) in PM_{10} with respect to their crustal abundances [25,26] were calculated using Fe as the reference element:

$$\text{Enrichment factor}\ (X) = \frac{[X]_{PM_{10}}/[Fe]_{PM_{10}}}{[X]_{crust}/[Fe]_{crust}}$$

Iron was chosen over Al and Si (which are other potential crustal reference elements) to avoid interferences from aluminosilicate (zeolite) catalysts arising from local petrochemical sources in Houston [27,28] (see next section). Further, iron was chosen as a reference as previous work has shown that even in industrialized

regions, it is highly correlated with other crustal elements such as silicon, indicating that the dominant source for this metal is dust resuspension [29]. Median values of the enrichment factors for Na, Mg, Al, Si, K, Sc, Ti, Mn, Co, Ga, Rb, Sr, Zr, Cs, Ba, and lanthanoids were close to unity suggesting that these elements in airborne PM_{10} originated predominantly from crustal rich sources, which may include soil entrainment and road dust resuspension. In contrast, median enrichment factors for Ca, V, Cr, Ni, Cu, Zn, As, Se, Mo, Sn, Sb, and Pb were much higher ranging between 8 and 875. Elevated enrichment factors for these metals, some of which are considered hazardous air pollutants by the United States Environmental Protection Agency, have also been reported from other industrialized areas around the world including South Korea (V, Ni, Cr, As, Zn, Pb, Sb and Se) [18], northern France (As, Co, Cr, Ni, and V) [20], Turkey (Cr, Ni, Zn, Mo, Se, As and Sb) [30], Singapore (Cr, Ni, Cu, Pb, Zn and V) [6], Italy (As, Cu, Mo, Ni, Pb, Sb, V and Zn) [19], Spain (Ni, V, Cr, As, Sb, Sn, Cu, Zn and Pb) [31] and New Zealand (Ca, Ni, Zn, As and Pb) [32] demonstrating the importance of anthropogenic sources for these elements.

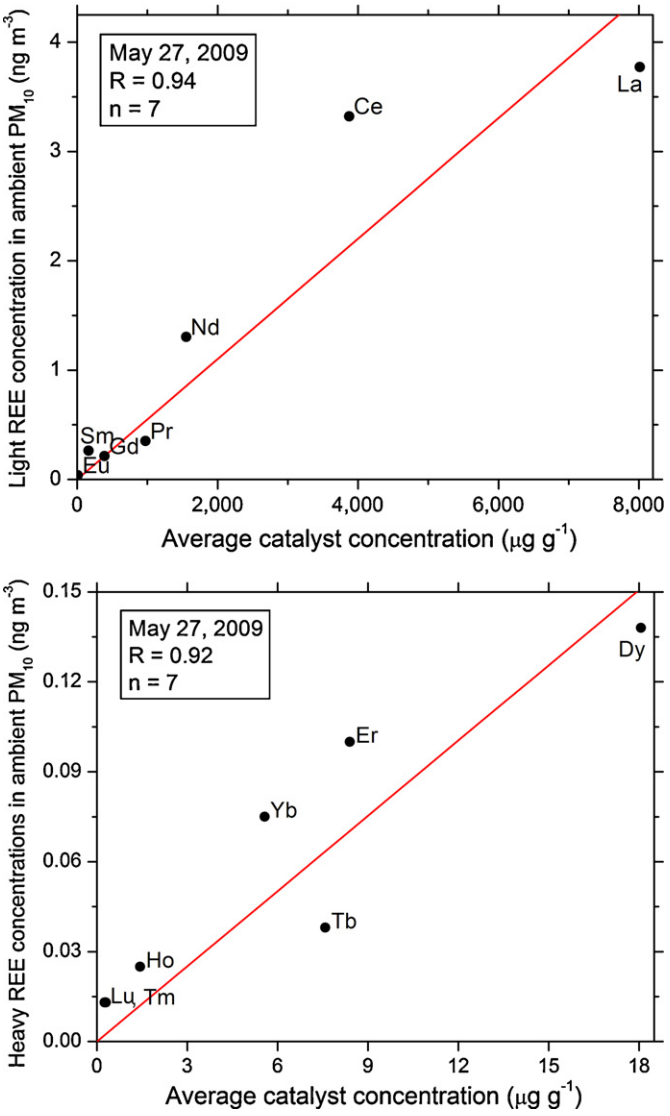

Fig. 5. Strong correlations between light and heavy lanthanoid concentrations in ambient PM_{10} and corresponding average values measured in fluidized bed cracking catalysts [27].

3.5. Identifying episodic emissions (i.e. industrial upsets)

The median La/Ce ratio in PM_{10} over the duration of sample collection was <1 (=0.62) indicating that overall lanthanoid enrichment was primarily caused by crustal resuspension and motor vehicle emissions [27,33]. However, La/Ce ratios in a small fraction of the samples were >1 as it is in source samples from refinery cracking catalysts [27,34]. Also, the heavy lanthanoids Tm and Lu were almost always below their detection limit (0.018 ng m^{-3}), but were detected infrequently. These same PM_{10} samples also exhibited elevated concentrations of all lanthanoids, typically 10–20-fold higher than the median value. These observations suggest episodic releases of fluidized bed catalytic cracking catalysts from petroleum refineries located in the vicinity of the sampling site that are greater than the "routine" emissions levels [28].

One such sample (collected on May 27, 2009 between 12:00 noon and 6:00 pm Central Daylight Time) with elevated lanthanoid concentrations was selected for further analysis. Note that process upsets are expected due to the complex nature of petroleum refining technology, especially during startup, shutdown, flaring, equipment malfunctions, poor maintenance practices and communication, etc. releasing catalyst particles to the atmosphere [35,36]. Since lanthanoids are specifically exchanged onto zeolites to increase hydrothermal stability and the yield of higher value products such as gasoline, they are excellent markers for such primary particulate emissions [23,28,34,37].

To identify a possible source of the elevated lanthanoids, the concentrations from the May 27, 2009 sample collected between 12:00 noon and 6:00 pm Central Daylight Time were strongly and positively correlated with corresponding average values measured in refining catalysts [27], as shown in Fig. 5. Further, the abundance sequence of the major lanthanoids was identical in the catalysts and this particular PM_{10} sample (La > Ce > Nd > Pr > Gd ~ Sm > Dy). Finally, enrichment factors for all light lanthanoids with respect to their average concentrations in cracking catalysts using Nd as the reference (the choice of Nd has been explained in Ref. [23]) were all close to unity. Therefore, fluidized-bed cracking catalysts appear to be primarily responsible for lanthanoid enrichment in this sample, and as a result, higher airborne particulate lanthanoid concentrations can be directly attributed to an air emissions event in one of the local refineries that released catalyst particles from the fluid catalytic cracking unit to the local atmosphere. Further, wind direction during the period of sample collection varied with wind blowing from the south, west and north [38]. This fluctuation in wind direction decreases the likelihood that long range transport from a distant source is responsible for the observed increase in PM concentration. Along with lanthanoids, concentrations of selected

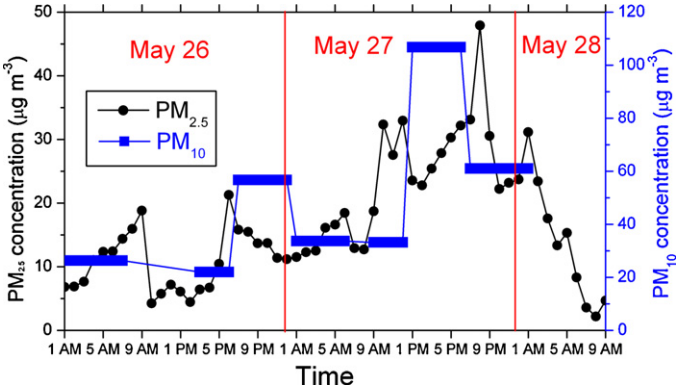

Fig. 6. Elevated $PM_{2.5}$ and PM_{10} concentrations during evening and night of May 27 at the Clinton Drive continuous ambient monitoring station supporting the hypothesis of an unreported particulate matter emission event [39].

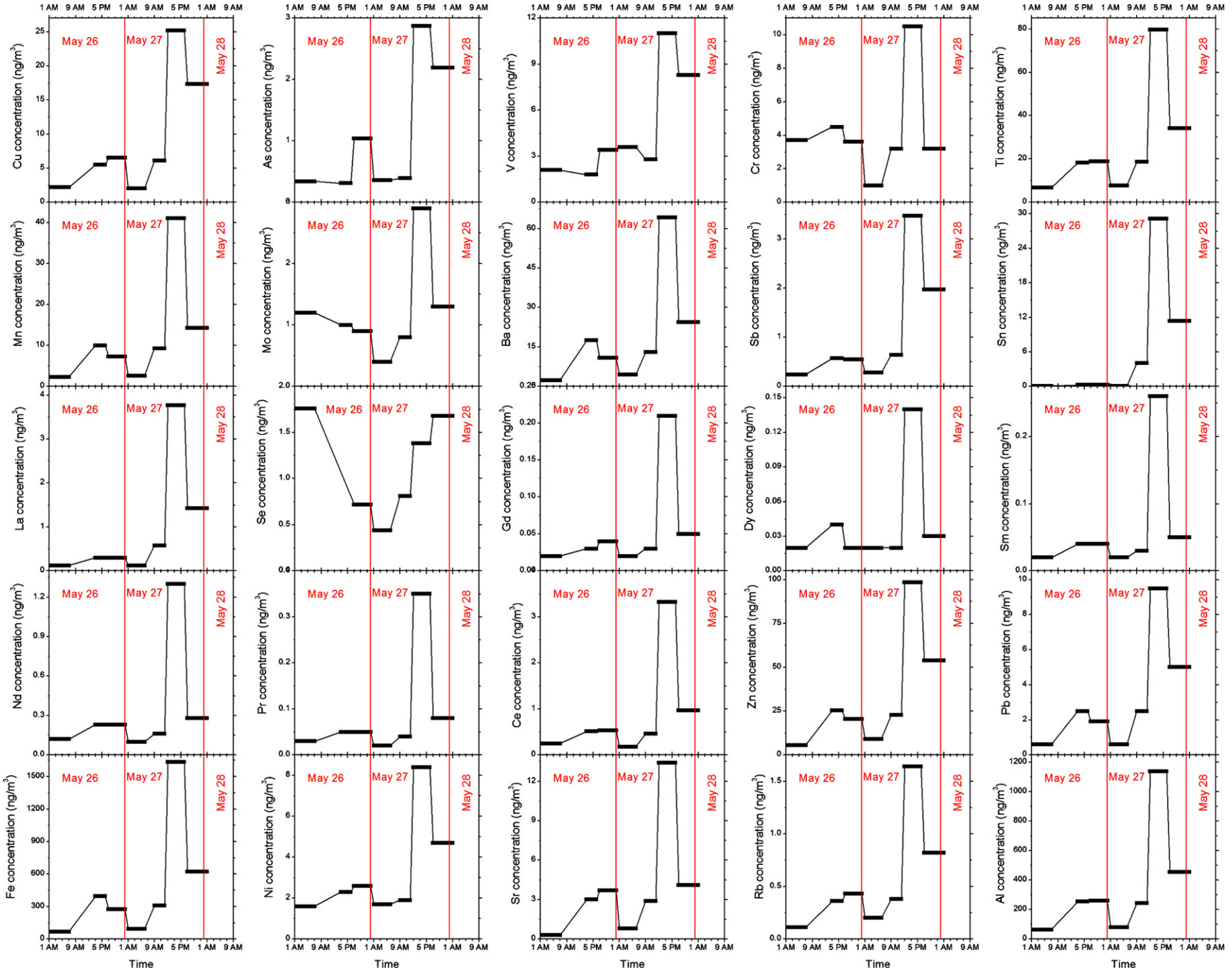

Fig. 7. Time series of 25 elements, including lanthanoids, during the time period of the episodic release showing their in-phase behavior (except Se) and elevated concentrations synchronous with the PM_{10} mass in Fig. 6.

transition metals especially Zn, Ni, and V were also substantially greater in this sample compared to those collected on other days. The Ni/V ratio was approximately conserved in the PM_{10} sample compared with NIST Fuel Oil SRM 1634c (0.62 and 0.76, respectively) lending further evidence for anthropogenic contributions.

Regulatory ambient PM monitoring conducted by the Texas Commission on Environmental Quality at Clinton Drive [39] showed that the apparent emission of material from a local fluidized bed catalytic cracking unit is concurrent with a significant increases in $PM_{2.5}$ levels over the evening hours of May 27 as depicted in Fig. 6. As regulatory PM_{10} sampling at Clinton Drive was not performed during this time period, the PM_{10} mass determined by the current sampling campaign is also shown in Fig. 6. Note that peak concentrations of fine and coarse PM are not exactly concurrent, probably induced by differences between sampling apparatus (TEOM for $PM_{2.5}$ and batch weighing for Teflon filters for PM_{10}) as well as differences in the atmospheric transport and deposition of coarse and fine PM.

Elevated PM levels in the evening are not common in Houston with peak $PM_{2.5}$ concentrations typically occurring during the early morning commute hours [40]. The elevated coarse PM sample shows strong enrichment of many metals including those associated with crustal sources (i.e. Al, Fe, Ti), combustion sources (i.e. V, Pb, Ni), mobile sources (i.e. Ba), and FCC emissions (i.e. lanthanoids). Regulatory monitoring programs commonly rely on ED-XRF for speciation, a technique that typically is best suited only for the high concentration elements (e.g. Al, Si, Fe). Hence, elevated levels of only the high concentration crustal minerals in the evening of May 27 (Fig. 7) might be misinterpreted to suggest the elevated PM is of natural (crustal) origin. The likely impact of industrial emissions over this period is revealed only by the detailed trace-level multi-elemental analysis showing correlations between ambient concentrations and source composition of FCC catalyst (Fig. 5) along with the in-phase behavior of many other metals with lanthanoids (Fig. 7). The simultaneous increase of numerous metals may indicate multiple sources, but FCC catalysts also have high concentrations of crustal minerals (originating from the ore used to form the zeolite support structure), REEs (originating from the zeolite catalyst doping), and V and Ni (originating from crude oil which is cracked by these catalysts).

Further, Fig. 7 depicts that profiles of each of the measured lanthanoids (La, Ce, Pr, Nd, Sm, Gd and Dy) were in phase, following each other very closely, and even peaking at the same date and time as the coarse PM sample (as shown in Fig. 6) and many other main group and transition metals. Additional evidence for a common emission source (FCC catalysts) comes from statistically significant and positive correlations ($p = 0.01$) between each of these lanthanoids during this time frame.

La/V has been reported to be >1 in ambient $PM_{2.5}$ samples collected during a significant FCC episode [28]. In contrast, La/V ratio for this ambient PM_{10} sample was only 0.32 (similar to pristine soils) demonstrating a confounding effect from other non-refining sources that are relatively rich in vanadium such as coal and oil combustion and crustal material. Hence, La/V ratios alone may only be of limited value in identifying direct refinery contributions in heavily industrialized locations [37] including the Houston Ship Channel region. Additionally, La/Ce in this PM_{10} sample was 1.1, which is significantly lower than the range reported for $PM_{2.5}$ during episodes (3.2–5.6) and in "background" concentrations (2.5–7.2) [27,28]. Substantially lower ratios of La/V and La/Ce in PM_{10} demonstrate significant contributions from non-refinery sources such as soil resuspension, oil combustion, and motor vehicles which are known to impact coarse PM at this site [40].

Concentrations of Se, commonly linked to coal combustion [41], do not show similar temporal patterns as other elements (including on May 27) as shown in Fig. 7 demonstrating the complex interrelationships between different sources contributing to PM at this site.

3.6. Implications for air quality management in southeast Texas

This PM emission event reported here is probably less severe than another FCC episode tracked recently [28], since (i) ambient lanthanoid concentrations were 5–15 times lower during the current study and (ii) a lower La/V ratio of 0.32 was measured in this study compared to the value of 1.8 reported earlier. Nevertheless, our measurements indicate that it contributed substantially to local $PM_{2.5}$ concentrations, which peaked at $\sim 50\,\mu g\,m^{-3}$, at an unusual time (8 pm local time), and the elevated $PM_{2.5}$ levels during this period were previously unaccounted for. Additionally, there are no official reports of particulate matter releases from nearby sources on May 26 and May 27, 2009 in the Air Emission Event Database of the Texas Commission on Environmental Quality [42] even though unauthorized emissions of volatile organic compounds, CO, SO_2, NO_x, and H_2S were reported by BASF and ExxonMobil [43,44]. Hence, the particulate matter em ission event identified in Section 3.5 appears to be an unreported one. This is consistent with existing evidence of systematic underreporting of emissions from industrial sources, e.g. [45,46] and underscores the need for, and importance of independent environmental monitoring. Since other instrumental techniques are not well suited for trace level detection of multiple elements in atmospheric PM at high throughput, ICP-MS measurements are imperative to better characterize and identify industrial emission events. This will provide the scientific basis for industry compliance with existing regulations and augment existing self-reporting of emission events. Further, better understanding of aerosol chemical composition, the role of metals in heterogeneous particle formation, and variability in emissions will advance the development of effective strategies to improve air quality in urban, industrialized regions. Existing evidence suggests that controlling episodic emissions of volatile organic compounds maybe more effective in controlling local ozone concentrations compared with reducing routine emissions [47]. In a similar manner, limiting episodic particulate matter emissions can also be expected to restrict overall PM levels within acceptable limits.

4. Conclusions

A robust procedure incorporating NH_3 as a reaction gas was developed to make accurate and precise measurements of several metals (Al, Fe, Ni, Cr, Cu, V, and Zn) in numerous coarse airborne PM samples using DRC-q-ICP-MS. The reaction cell technique greatly improved V and Cr detection and provided modest improvements for Al, Fe, Ni, Cu, and Zn when a combination of HNO_3, HF, and H_3BO_3 was used for sample digestion. The other 37 elements (including lanthanoid metals) were also analyzed by q-ICP-MS in the standard mode (i.e. without NH_3). It is anticipated that the reaction cell approach will be even more valuable being able to reduce a wider range of (potentially more severe) interferences when HCl is also employed during microwave digestion as is necessary for platinum group metals. This is the subject of our on-going research, which focuses on adapting DRC techniques to simultaneously measure a broad suite of elements including those from the platinum group, lanthanoids, and others reported in this paper in order to better quantify contributions of both mobile and industrial sources to atmospheric particulate matter.

Importantly, using DRC-q-ICP-MS measurements, we were able to measure and monitor an unreported, transient anthropogenic PM emission episode which contributed to higher particulate matter levels in Houston, TX. Based on our findings reported herein,

we recommend long-term independent monitoring of aerosols and trace elemental speciation with ICP-MS especially in industrial areas. This would be particularly useful towards air quality management efforts as well as providing data to better evaluate the metals hypothesis for adverse health effects associated with airborne PM [48].

Acknowledgments

This project has been funded by the Environmental Protection Agency, by the State of Texas as part of the program of the Texas Air Research Center, and by the Environmental Institute of Houston. The contents do not necessarily reflect the views and policies of the sponsor nor does the mention of trade names or commercial products constitute endorsement or recommendation for use. We thank Steven Paciotti of the Texas Commission on Environmental Quality for assisting with sample collection. We also appreciate the assistance of Peter Deng, Pranav Kulkarni, Allison Pekkanen, and Mutiara Ayu Sari during the course of this research.

Appendix A. Supplementary data

Supplementary data associated with this article can be found, in the online version, at doi:10.1016/j.aca.2010.11.037.

References

[1] C.I. Davidson, R.F. Phalen, P.A. Solomon, Aerosol Science and Technology 39 (2006) 737.
[2] C.A. Pope, M. Ezzati, D.W. Dockery, The New England Journal of Medicine 360 (2009) 376.
[3] C.S. Claiborn, T. Larson, L. Sheppard, Environmental Health Perspectives 110 (2002) 547.
[4] M.E. Gerlofs-Nijland, M. Rummelhard, A.J.F. Boere, D.L.A.C. Leseman, R. Duffin, R.P.F. Schins, P.J.A. Borm, M. Sillanpaa, R.O. Salonen, F.R. Cassee, Environmental Science and Technology 43 (2009) 4729.
[5] J.G. Watson, J.C. Chow, C.A. Frazier, X-ray fluorescence analysis of ambient air samples, in: S. Landsberger, M. Creatchman (Eds.), Elemental Analysis of Airborne Particles, Gordan and Breach Science Publisher, Amsterdam, The Netherlands, 1999, p. 67.
[6] R. Balasubramanian, W.B. Qian, Journal of Environmental Monitoring 6 (2004) 813.
[7] N.J. Pekney, C.I. Davidson, Analytica Chimica Acta 540 (2005) 269.
[8] K. Swami, C.D. Judd, J. Orsini, K.X. Yang, L. Husain, Fresenius' Journal of Analytical Chemistry 369 (2001) 63.
[9] S. Karthikeyan, U.M. Joshi, R. Balasubramanian, Analytica Chimica Acta 576 (2006) 23.
[10] S.D. Tanner, V.I. Baranov, D.R. Bandura, Spectrochimica Acta Part B: Atomic Spectroscopy 57 (2002) 1361.
[11] S. D'Ilio, N. Violante, S. Caimi, M. Di Gregorio, F. Petrucci, O. Senofonte, Analytica Chimica Acta 573–574 (2006) 432.
[12] B.L. Batista, J.L. Rodrigues, J.A. Nunes, V.C. de Oliveira Souza, F. Barbosa Jr., Analytica Chimica Acta 639 (2009) 13.
[13] Y.-J. Tseng, Y.-D. Tsai, S.-J. Jiang, Analytical and Bioanalytical Chemistry 387 (2007) 2849.
[14] C.-Y. Kuo, S.-J. Jiang, A.C. Sahayam, Journal of Analytical Atomic Spectrometry 22 (2007) 636.
[15] A.J. Bednar, R.A. Kirgan, W.T. Jones, Analytica Chimica Acta 632 (2009) 27.
[16] P.E. Rasmussen, A.J. Wheeler, N.M. Hassan, A. Filiatreault, M. Lanouette, Atmospheric Environment 41 (2007) 5897.
[17] S.F. Kan, P.A. Tanner, Atmospheric Environment 39 (2005) 2625.
[18] J.-M. Lim, J.-H. Lee, J.-H. Moon, Y.-S. Chung, K.-H. Kim, Atmospheric Research 96 (2010) 53.
[19] G. Dongarrà, E. Manno, D. Varrica, M. Vultaggio, Atmospheric Environment 41 (2007) 7977.
[20] L. Lamaison, L.Y. Alleman, A. Robache, J.-C. Galloo, Applied Spectroscopy 63 (2009) 87.
[21] P. Kulkarni, S. Chellam, J.B. Flanagan, R.K.M. Jayanty, Analytica Chimica Acta 599 (2007) 170.
[22] J.W. Olesik, D.R. Jones, Journal of Analytical Atomic Spectrometry 21 (2006) 141.
[23] P. Kulkarni, S. Chellam, D.W. Mittlefehldt, Analytica Chimica Acta 581 (2007) 247.
[24] S.D. Tanner, V.I. Baranov, Journal of the American Society of Mass Spectrometry 10 (1999) 1083.
[25] S.R. Taylor, S.M. McLennan, The Continental Crust: Its Composition and Evolution. An Examination of the Geochemical Record Preserved in Sedimentary Rocks, Blackwell Scientific, Oxford, 1985.
[26] R.L. Rudnick, S. Gao, Composition of the continental crust, in: H.D. Holland, K.K. Turekian (Eds.), Treatise on Geochemistry, Elsevier/Pergamon, Boston, MA, 2004, p. 1.
[27] P. Kulkarni, S. Chellam, M.P. Fraser, Atmospheric Environment 40 (2006) 508.
[28] P. Kulkarni, S. Chellam, M.P. Fraser, Environmental Science and Technology 41 (2007) 6748.
[29] M. Singh, P.A. Jacques, C. Sioutas, Atmospheric Environment 36 (2002) 1675.
[30] G. Güllü, G. Dogan, G. Tuncel, Atmospheric Environment 39 (2005) 6376.
[31] J. Pey, X. Querol, A. Alastuey, Atmospheric Environment 44 (2010) 1587.
[32] I. Senaratne, D. Shooter, Atmospheric Environment 38 (2004) 3049.
[33] X. Huang, I. Olmez, N.K. Aras, Atmospheric Environment 28 (1994) 1385.
[34] I. Olmez, G.E. Gordon, Science 229 (1985) 966.
[35] F.G. Wolf, Production and Operations Management 10 (2001) 292.
[36] J.H. Gary, G.E. Handwerk, M.J. Kaiser, Petroleum Refining: Technology and Economics, CRC Press, Boca Raton, FL, 2007.
[37] T. Moreno, X. Querol, A. Alastuey, W. Gibbons, Atmospheric Environment 42 (2008) 7851.
[38] Texas Commission on Environmental Quality, Texas Air Monitoring Information System (TAMIS) dataset (accessed 22.10.10).
[39] Texas Commission on Environmental Quality, PM2.5 data: soot, dust, smoke (fine particulate matter). http://www.tceq.state.tx.us/cgi-bin/compliance/monops/monthly_summary.pl (accessed 15.08.10).
[40] M. Russell, D.T. Allen, D.R. Collins, M.P. Fraser, Aerosol Science and Technology 38 (2004) 14.
[41] J.G. Watson, J.C. Chow, J.E. Houck, Chemosphere 43 (2001) 1141.
[42] Texas Commission on Environmental Quality, Austin, http://www11.tceq.state.tx.us/oce/eer/index.cfm (accessed 17.06.10).
[43] Texas Commission on Environmental Quality, Reports of air emission events (number: 124530), Austin, Texas. http://www.tceq.state.tx.us/compliance/field_ops/eer (accessed 18.06.10).
[44] Texas Commission on Environmental Quality, Reports of air emission events (numbers: 124725, 124689, 124761), Austin, Texas. http://www.tceq.state.tx.us/compliance/field_ops/eer (accessed 18.06.10).
[45] U.S. House of Representatives, Oil refineries fail to report millions of pounds of harmful emissions (available from http://southdakota.sierraclub.org/LivingRiver/Waxman%20oil%20refineries.pdf), prepared for Rep. Henry A. Waxman. Document 20040827114147-65907.
[46] Environmental Integrity Project and the Galveston–Houston Association for Smog Prevention, Who's counting? The systematic underreporting of toxic air emissions (available from http://www.environmentalintegrity.org/pdf/publications/TRIFINALJune_22.pdf), Houston, TX.
[47] J. Nam, M. Webster, Y. Kimura, H. Jeffries, W. Vizuete, D.T. Allen, Atmospheric Environment 42 (2008) 4198.
[48] K. Sexton, S.H. Linder, D. Marko, H. Bethel, P.J. Lupo, Environmental Health Perspectives 115 (2007) 1388.